Review Article   **Open Access**

Y. Fang, C. T. Wolowiec, D. Yazici, and M. B. Maple*

Chemical Substitution and High Pressure Effects on Superconductivity in the LnOBiS$_2$ (Ln = La-Nd) System

Abstract: A large number of compounds which contain BiS$_2$ layers exhibit enhanced superconductivity upon electron doping. Much interest and research effort has been focused on BiS$_2$-based compounds which provide new opportunities for exploring the nature of superconductivity. Important to the study of BiS$_2$-based superconductors is the relation between structure and superconductivity. By modifying either the superconducting BiS$_2$ layers or the blocking layers in these layered compounds, one can effectively tune the lattice parameters, local atomic environment, electronic structure, and other physical properties of these materials. In this article, we will review some of the recent progress on research of the effects of chemical substitution in BiS$_2$-based compounds, with special attention given to the compounds in the LnOBiS$_2$ (Ln = La-Nd) system. Strategies which are reported to be essential in optimizing superconductivity of these materials will also be discussed.

Keywords: BiS$_2$-based compounds, superconductivity, rare earth materials

*Corresponding Author: M. B. Maple: Department of Physics, Materials Science and Engineering Program, and Center for Advanced Nanoscience, University of California, San Diego, La Jolla, California 92093, USA, E-mail: mbmaple@ucsd.edu
Y. Fang: Materials Science and Engineering Program and Center for Advanced Nanoscience, University of California, San Diego, La Jolla, California 92093, USA
C. T. Wolowiec: Department of Physics and Center for Advanced Nanoscience, University of California, San Diego, La Jolla, California 92093, USA
D. Yazici: Department of Physics and Center for Advanced Nanoscience, University of California, San Diego, La Jolla, California 92093, USA

1 Introduction

Following the discovery of superconductivity by Kammerlingh Onnes in 1911, efforts in the search for new superconducting materials during the past century have shown that most of the pure metals and an enormous number of alloys and compounds become superconducting at low temperatures. The highest superconducting critical temperature T_c that has been reported is 133 K for the cuprates at ambient pressure and 203 K in sulfur hydride at 155 GPa, although the latter claim has not yet been independently verified [1, 2]. In order to experimentally realize new superconducting materials with properties suitable for practical applications, there is still much to accomplish in both theory and experiment. The recently discovered family of BiS$_2$-based superconductors exhibit a layered crystal structure which is characterized by an alternating pattern of BiS$_2$ double layers that are separated by blocking layers [3]. This layered structure provides new hope and opportunity to enrich the class of layered superconductors with higher values of T_c.

Chemical substitution may induce significant change in materials to their lattice parameters, crystal structure and electronic structure. It has been broadly used as a strategy to tune physical properties of materials including electronic transport, magnetic, thermal, mechanical, and luminescent properties. Chemical substitution has been found to induce superconductivity via electron or hole doping in LnFeAsO compounds by replacing F for O [4–10], Co for Fe [11], Sr for La [12], Th for Gd [13], and also through the introduction of oxygen vacancies [14, 15]. Similar to the LnFeAsO compounds, it has been reported that electron carriers are essential for the emergence of superconductivity in the BiS$_2$-based materials [3, 16]. By modifying the blocking layers of the BiS$_2$-based compounds, electron carriers can be generated within the structures. As a result, many of novel BiS$_2$-based superconductors, such as Bi$_4$O$_4$S$_3$, Bi$_3$O$_2$S$_3$, LnO$_{1-x}$F$_x$BiS$_2$ (Ln = La, Ce, Pr, Nd, Yb), La$_{1-x}$$M_x$OBiS$_2$ (M = Ti, Zr, Hf, Th), Sr$_{1-x}$La$_x$FBiS$_2$,

$EuBiS_2F$, and $Eu_3Bi_2S_4F_4$, have been developed with values of T_c ranging from 2.7 to 10.6 K [3, 10, 17–26].

The superconducting properties of BiS_2-based compounds are also sensitive to the environment in which they are synthesized or being measured. For example, polycrystalline samples of $LaO_{1-x}F_xBiS_2$ subjected to high pressure (HP) annealing have T_c values significantly higher than as-grown (AG) samples. Also, with the application of external hydrostatic pressure, a monotonic decrease in T_c is observed for both the $Bi_4O_4S_3$ and $SrFBiS_2$ compounds [27, 28]; in contrast, the compounds $LnO_{1-x}F_xBiS_2$, $Eu_3Bi_2S_4F_4$, $EuFBiS_2$, $LaO_{0.5}F_{0.5}BiSe_2$ and $Sr_{0.5}La_{0.5}FBiS_2$ were reported to have a sharp jump in T_c under applied pressure, indicating a pressure-induced transition from a low-T_c to high-T_c superconducting phase [27, 29–34]. It is also observed that superconductivity in the BiS_2-based compounds is very sensitive to chemical composition and to the level of electron doping in particular. As a result, T_c values of the samples with the same nominal chemical composition are not always the same since there might be slight differences in the actual chemical composition.

At present, there have been more than one hundred research papers published regarding superconductivity in the BiS_2-based compounds, which have helped increase our understanding of these novel materials and superconductivity in general. The peculiar crystal structure of these BiS_2-based compounds as a landscape for studying and optimizing superconductivity has fostered a healthy competition within the scientific community to explore the important critical parameters that affect T_c as well as to understand the nature of superconductivity itself in these layered structures. In this article, we will review some of the recent progress in both the study of chemical substitution and external pressure effects on the BiS_2-based compounds. Discussions about some of the parameters that are essential for superconductivity in these compounds will also be presented.

2 $Bi_4O_4S_3$

As the first discovered superconductor in the BiS_2-based compounds, $Bi_4O_4S_3$ is a bulk superconductor with a T_c of about 4.5 K [3, 35]. The structure of $Bi_4O_4S_3$ is derived from the structure of the parent $Bi_6O_8S_5$ with a 50% deficiency in SO_4 units; this results in the presence of electron carriers in the BiS_2 layers which induce the superconductivity in $Bi_4O_4S_3$ [3, 36]. Interestingly, the parent phase, $Bi_6O_8S_5$, which was initially regarded as a band insulator,

was soon found to show superconductivity at $\sim$4.2 K when the sample is annealed in vacuum [37].

Chemical substitutions have been found to suppress T_c in the superconducting compound $Bi_4O_4S_3$. Substitution of Se at the S site results in a slight increase in the lattice parameter c and a remarkable enhancement of the normal state resistivity [38]. The T_c of the $Bi_4O_4S_{3-x}Se_x$ compound decreases with increasing Se concentration from 4.4 K at $x = 0$ to 3.5 K at $x = 0.15$, while the upper critical field at 0 K, $H_{c2}(0)$, determined by fitting the conventional one-band Werthamer–Helfand–Hohenberg (WHH) equation to the $H_{c2}(T)$ data, is also suppressed from 2.3 to 1.8 T [39]. Similarly, T_c of the $Bi_{4-x}Ag_xO_4S_3$ compound gradually decreases with increasing Ag concentration and a subtle shrinkage of both the a and c lattice parameters were observed up to $x = 0.2$ [40]. It should be noted that the chemical pressure generated by Ag substitution is negligible in $Bi_4O_4S_3$ and the suppression of T_c most likely arises from the substitution of the Ag ions into the superconducting BiS_2 layers and the resultant change in the electronic structure of the compound.

3 $LnO_{1-x}F_xBiS_2$ (Ln = La, Ce, Pr, Nd, Yb)

The parent compounds in the $LnOBiS_2$ family are band insulators. The substitution of F for O induces superconductivity via electron doping into the BiS_2 layers. By applying relatively small magnetic fields ($\sim$1 T) to polycrystalline specimens of these superconductors, the superconducting state can be destroyed [21]. Due to the chemical similarity of the rare earth elements, there is considerable flexibility in modifications that can be made to the blocking layers of these compounds which facilitates the investigation of the superconducting and normal state properties of BiS_2-based compounds. The $LnOBiS_2$ compounds crystallize in a tetragonal structure with space group $P4/nmm$ [20]. Between each LnO blocking layer, there is a double BiS_2 superconducting layer in which there are two distinct positions for the S ions: in-plane position (S1) and out-of-plane position (S2), as indicated in Fig. 1.

Currently, superconductivity has been induced in five different parent compounds Ln(O,F)BiS_2 (Ln = La, Ce, Pr, Nd, Yb), with the substitution of F for O [21]. Polycrystalline samples of these compounds can be synthesized by using solid state reactions in sealed quartz tubes. However, along with the main superconducting phase, small amounts of secondary phases including LnF_3 and BiF_3 may also be formed in the polycrystalline samples [10, 19–
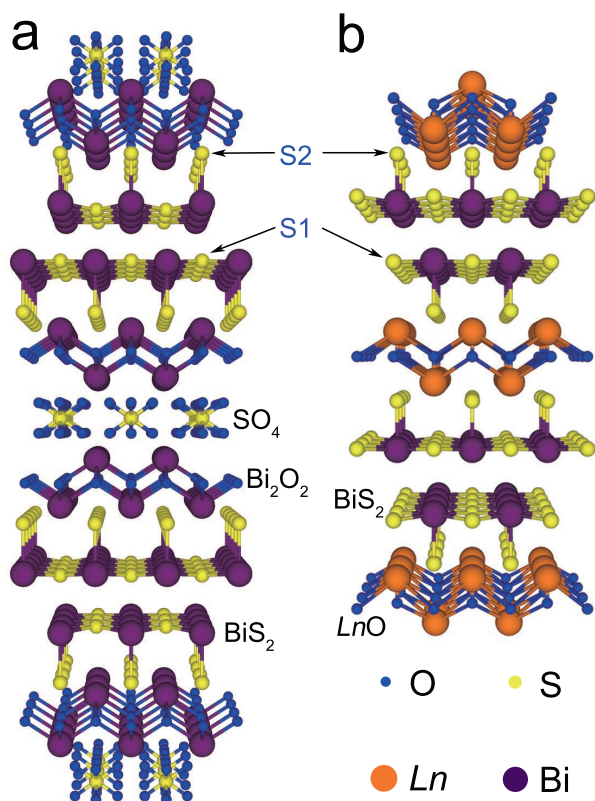
Figure 1: (Color online) Representative crystal structure of (a) Bi$_4$O$_4$S$_3$ and (b) LnOBiS$_2$. O^{2-} ions in the LnO blocking layer can be partially replaced by F$^-$. S1 and S2 indicate the in-plane and out-of-plane positions of S, respectively, in the superconducting BiS$_2$ layers of the two structures.

diagram of the BiS$_2$-based superconductors is still a significant challenge in research on BiS$_2$-based superconductors [44].

3.1 Electronic and crystal structures, and their correlation with T_c
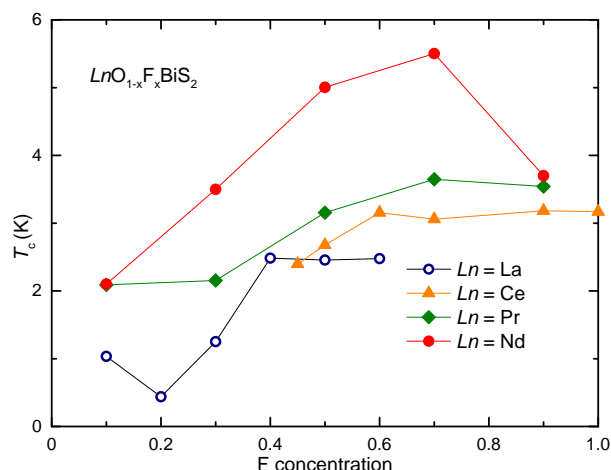
Figure 2: (Color online) Dependence of T_c on nominal F concentration for LnO$_{1-x}$F$_x$BiS$_2$ (Ln = La-Nd). The T_c values for Ln = La, Ce, Pr, Nd are obtained from Ref. [45–48], respectively. For interpretation of the definition of T_c of each sample, the reader is referred to the corresponding articles.

21, 41, 42]. As a result, the actual chemical composition of these compounds may be different from the nominal chemical composition, particularly regarding the concentration of F, resulting in an overestimated level of electron doping into the BiS$_2$ layers. This concern has also been raised in the study of single-crystalline samples of NdO$_{1-x}$F$_x$BiS$_2$, in which case, the actual electron doping level was reported to be much lower than anticipated [43]. Hence, T_c values of samples with the same nominal chemical composition reported by different authors may differ from one another [21, 22]. Although conclusive evidence of inhomogeneity in polycrystalline samples of the BiS$_2$-based superconductors has not been reported, measurements of electrical resistivity (ρ), magnetic susceptibility (χ), and specific heat (C), etc. may still be partially affected by possible inhomogeneity of the samples, and thus compromise reports of some of the intrinsic properties of these compounds. In addition, the existence of defects and disorder in these materials may also complicate the analysis of experiments and comparison with theoretical models. As mentioned by Kuroki, establishing the intrinsic phase

The T_c vs x plots for LnO$_{1-x}$F$_x$BiS$_2$, displayed in Fig. 2, show a broad range of F concentration in which superconductivity can be induced; there is also an apparent enhancement of T_c with increasing Ln atomic number. The optimal F concentration for superconductivity in these compounds falls within the range of $0.4 \leqslant x \leqslant 0.7$. As the concentration of F is increased, the superconductivity of these compounds was also found to be more resistant to the destructive effects of an external magnetic field up to the F solubility limit [47, 48]. As an example, the upper critical field of NdO$_{1-x}$F$_x$BiS$_2$ increases from 0.9 T at x = 0.3 to 3.3 T at x = 0.7 [48]. For LaO$_{1-x}$F$_x$BiS$_2$, first-principles calculations suggest that the density of states at the Fermi level increases with increasing F substitution and attains its maximum value at x = 0.5 [16]. Hence, a large number of studies have been made on compounds with a nominal composition given by LnO$_{0.5}$F$_{0.5}$BiS$_2$ [10, 19, 20].

Electronic structure calculations for LnO$_{1-x}$F$_x$BiS$_2$, and, in particular, for the compound LaO$_{0.5}$F$_{0.5}$BiS$_2$, have been widely reported [49, 50]. It was suggested that LaOBiS$_2$ is an insulator with an energy gap of $\sim$0.8 eV [51],
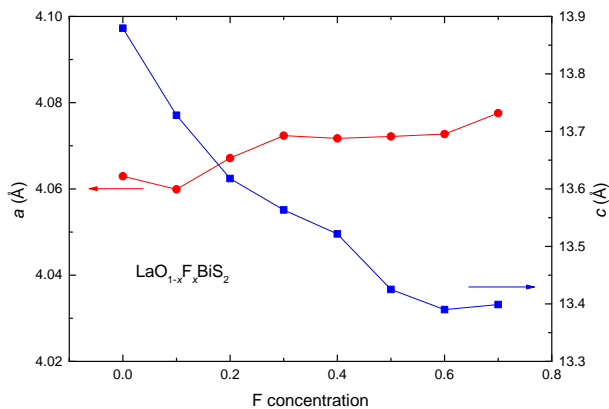
Figure 3: (Color online) Nominal F concentration dependence of the lattice constants a (red) and c (blue) of AG $LaO_{1-x}F_xBiS_2$. The data are obtained from Ref. [24].

Figure 4: (Color online) (left) Crystal structure of $LaO_{0.5}F_{0.5}BiS_2$. (right) The side view of the BiS_2 layers for $x = 0$ and $x = 0.5$ is displayed in the top and bottom panel, respectively. Adapted with permission from Ref. [16]. Copyrighted by the American Physical Society.

which is consistent with experimental evidence revealing significantly high values of ρ and negative temperature coefficients ($d\rho/dT < 0$) in polycrystalline samples [52]. As F is substituted into the O site (see Fig. 1), it is expected that electrons will be doped into the conduction bands which consist mainly of Bi-$6p$ orbitals, resulting in an increase in charge carrier density in the BiS_2 layers [3, 50]. The possibility of conventional strong coupling s-wave superconductivity for $Bi_4O_4S_3$, $LaO_{0.5}F_{0.5}BiS_2$, and $NdO_{1-x}F_xBiS_2$ has been supported by measurements of magnetic penetration depth using muon-spin spectroscopy or tunnel diode resonator techniques [53–56]. In addition, some theoretical studies suggest that the superconductivity observed in the BiS_2-based compounds occurs via strong electron-phonon coupling [16, 51, 57]. However, other unconventional pairing mechanisms including extended s- or d-wave pairing, g-wave pairing, and triplet spin pairing were also proposed [58–62]. While evidence for both electron-phonon coupling [16, 51, 53–57] and strong electron-electron interactions [58–64] has been reported, the concentration of charge carriers in the BiS_2 layers is considered to be essential for the superconductivity in the $LnO_{1-x}F_xBiS_2$ compounds [18, 20, 21, 24, 27, 51, 52, 54, 65].

The substitution of F for O in $LnOBiS_2$ may also induce a change in lattice parameters due to the smaller size of the F^- ions compared with O^{2-} ions. For $LnO_{1-x}F_xBiS_2$, the length of the a-axis does not change significantly upon F substitution; however, the c-axis decreases monotonically until the F concentration reaches the solubility limit (typically around 50%) as illustrated by the example of $LaO_{1-x}F_xBiS_2$ shown in Fig.3 [10, 19, 20, 47, 48]. The highest value of T_c was reported when c attains its minimum value, and the evolution of T_c seems consistent with the change in lattice parameter c [20, 47, 48]. However, it
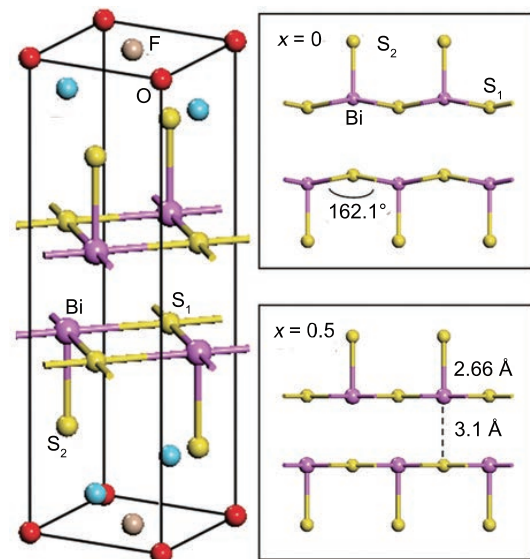
should be noted that these results do not necessarily indicate an exclusive role of the lattice parameter c in affecting T_c, since it is observed that the level of electron doping also reaches a maximum when the c parameter is smallest.

Local distortion of the lattice may also be induced by F substitution. Asymmetric broadening of the diffraction peaks with increasing F concentration in $LaO_{1-x}F_xBiS_2$ was observed in neutron scattering measurements, suggesting that strain may be induced along the c-axis due to a random substitution of the F ions at O sites [52]. It is also possible for a distortion to occur in the BiS_2 plane as a result of F substitution. For the $LaO_{1-x}F_xBiS_2$ compounds, first-principles calculations show that the z coordinate of the in-plane S and Bi atoms in the unit cell decreases with doping, yielding a nearly perfect planar structure at $x = 0.5$ (see Fig. 4). In fact, by using single crystal X-ray diffraction, nearly flat in-plane S-Bi-S angles were observed in $LaO_{1-x}F_xBiS_2$ at $x = 0.46$, which is close to the optimal F concentration value ($x = 0.5$) that yields the highest value of T_c [67, 68]. A flat Bi–S plane would result in an increase in hybridization of the p_x/p_y orbitals of Bi and S and, in turn, enhanced superconductivity. Investigation of extended X-ray absorption fine structure (EXAFS) of the $CeO_{1-x}F_xBiS_2$ compounds reveals that the local structure of both the BiS_2 superconducting layer and the Ce(O,F) blocking layer changes systematically with increasing F concentration [66]. The Bi-S2 distance increases with F concentration while the Ce-S2 distance decreases
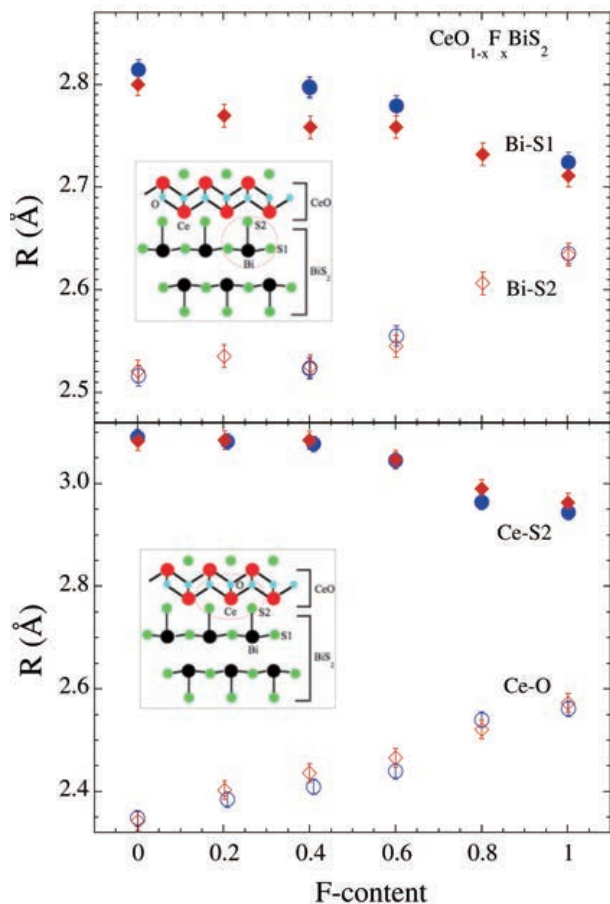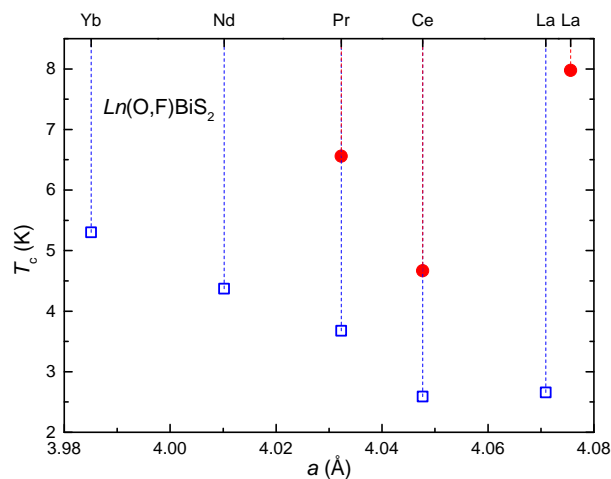
Figure 5: (Color online) Near-neighbor distances from Bi (upper) and Ce (lower) as a function of F concentration. Blue circles and red diamonds represent the data taken from the as-grown and high pressure annealed samples, respectively. The insets show structural cartoons with near-neighbour atomic clusters (encircled) around Bi and Ce. Reprinted with permission from Ref. [66]: Determination of local atomic displacements in CeO$_{1-x}$F$_x$BiS$_2$ system, J. Phys.: Condens. Matter 26 (2014) 435701. Copyright (2014) by the IOP Publishing.

Figure 6: (Color online) Correlation between T_c and a-axis of LnO$_{1-x}$F$_x$BiS$_2$ ($x = 0.5$ for Ln = La, Pr, Nd, Yb, $x = 0.3$ for Ln = Ce) superconductors. The open squares and filled circles represent the data obtained from as-grown samples and high pressure annealed samples, respectively. Dashed lines are guides to the eye. The T_c and a values for Ln = Nd, Yb samples are obtained from Ref. [21] and the data for Ln = La, Ce, Pr samples are taken from Refs. [65, 70, 71], respectively.

with F concentration (see Fig. 5), leading to the breaking of the Ce-S-Bi coupling channel [69]. Consequently, the hybridization between the Ce 4f orbital and the Bi-6p conduction band decreases with F concentration and the Ce^{3+}/Ce^{4+} valence fluctuations are suppressed, resulting in a completely localized 4f^1 (Ce^{3+}) state at $x > 0.4$, where the samples exhibit superconductivity and ferromagnetism [69]. Therefore, it has been suggested that the valence of Ce, i.e., the coupling between the Ce 4f and Bi 6p states, is not beneficial to the superconductivity.

Considering the contraction in radius for the Ln ions, one may expect changes in both lattice parameters a and c as well as changes in T_c with increasing atomic number of Ln. Figure 6 displays typical values of T_c, defined as the temperature at which ρ falls to 50% of its normal-state value, for the compounds in the Ln(O,F)BiS$_2$ system, as a function of lattice constant a. Except for the Ln = Yb and Nd cases, the T_c values of the samples after HP annealing are higher than the values of the AG samples. In addition, the dependence of T_c on the lattice paramter a for the AG samples is completely different from those of the HP annealed samples: for the AG samples, T_c increases with decreasing a (heavier Ln); however, the value of T_c for LaO$_{0.5}$F$_{0.5}$BiS$_2$ after HP annealing (a larger value of a) is significantly higher than the value of other HP annealed samples (smaller values of a). While the values of T_c for both AG and HP annealed samples appear to be correlated, although differently, with the length of the a-axis [36], no structural phase transition was observed by HP annealing and the lattice parameters a and c for the AG and HP annealed samples are similar; this suggests that there should be other factors which have a significant effect on T_c. The markedly different values in T_c between the AG and HP annealed samples currently has no satisfactory explanation. However, evidence of a local distortion in the lattice has been reported, and this distortion is likely to be a source of the difference in T_c. For the HP annealed samples of CeO$_{1-x}$F$_x$BiS$_2$, the in-plane Bi-S1 distance is shorter; however, the out-of-plane Bi-S2 distance and the sizing of the blocking layers appear to be marginally effected by the HP annealing (see Fig. 5) [66]. It was also suggested that the crystal structure within the ab plane of the CeO$_{0.3}$F$_{0.7}$BiS$_2$ compound evolved to a higher symmetry after HP anneal-

ing, resulting in a better tetragonal phase [70]. Finally, the uniaxial strain along the c-axis, which was found in annealed samples of the $LaO_{0.5}F_{0.5}BiS_2$ and $PrO_{0.5}F_{0.5}BiS_2$ compounds, was reported to be positively correlated with the enhancement of superconductivity [65, 71]. These results indicate that the optimization of the local structure is important for realizing higher T_c values in the BiS_2-based superconductors.

## 3.2 Normal state electrical resistivity, magnetic susceptibility, and specific heat
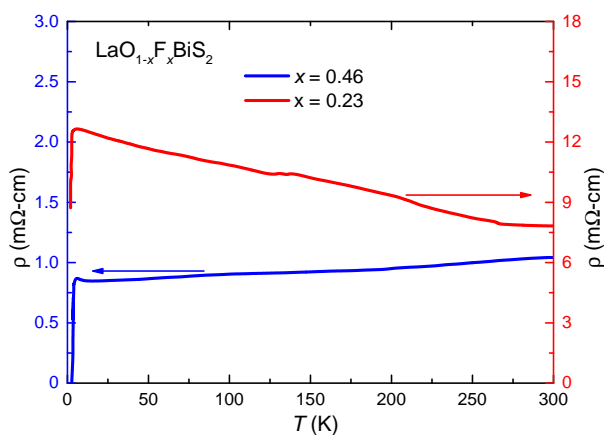
Figure 7: (Color online) Temperature dependence of the electrical resistivity, ρ, for $LaO_{1−x}F_xBiS_2$ ($x = 0.23$ and 0.46) single crystals. The data are obtained from Ref. [67].

Given that F substitution enhances the charge carrier density of BiS_2-based parent compounds, one would expect that F-substitution may induce more metallic-like behavior in these materials. The temperature dependence of $\rho(T)$ in the normal state for single crystals of $LaO_{1−x}F_xBiS_2$ ($x = 0.23, 0.46$) is shown in Fig. 7; while the crystal with $x = 0.23$ exhibits semiconducting-like behavior ($d\rho/dT < 0$), the crystal with $x = 0.46$ shows metallic behavior ($d\rho/dT > 0$) with significantly reduced values of resistivity [67]. These results are consistent with electronic band structure calculations which indicate that the parent compounds in this system should behave as band insulators but become metallic upon doping electron carriers into the BiS_2 layers [50]. However, the theoretical calculations do not fit well with measurements of $\rho(T)$ of polycrystalline samples of $LnOBiS_2$ which tend to exhibit strong sample dependent results. Some of the $LnOBiS_2$ parent compounds, which are in polycrystalline

form, have been reported to show semimetallic behavior in contrast to the semiconducting-like behavior of the corresponding F-doped polycrystalline samples [10, 25, 46–48]. However, this behavior may be related to the quality of these polycrystalline samples. For example, complete semiconducting-like behavior is reported in the case of $LaOBiS_2$ [52]; in addition, for the case of polycrystalline samples of $CeOBiS_2$, the resistivity can be significantly increased together with the appearance of semiconducting-like behavior after HP annealing [46].

Substitution of F into the lattice does not always result in a suppression of semiconducting-like behavior in polycrystalline samples. In fact, F substitution can enhance semiconducting-like behavior which has been observed in AG samples of $CeO_{1−x}F_xBiS_2$ and HP annealed samples of $LaO_{1−x}F_xBiS_2$ [10, 24]; this is in contrast to observations of suppressed semiconducting-like behavior by F substitution in single-crystalline samples of $CeO_{1−x}F_xBiS_2$ and $LaO_{1−x}F_xBiS_2$ [67, 72]. Although the cause of such unusual behavior is still unclear, the existence of grain boundaries as well as poor intergrain contacts in polycrystalline samples may contribute significantly to the semiconducting-like behavior of the F-substituted compounds. In addition to the semiconducting-metallic transition induced by F substitution in single crystals of $LaO_{1−x}F_xBiS_2$, research on single crystals of $NdO_{1−x}F_xBiS_2$ reveals metallic behavior in the normal state along the ab-plane of the crystal; this is different from the semiconducting behavior observed in polycrystalline samples of $NdO_{1−x}F_xBiS_2$ [43, 48, 64, 72, 73]. However, reports of the electrical transport properties in the normal state of single crystals of $CeO_{1−x}F_xBiS_2$ reveal semiconducting-like behavior in the ab-plane which is consistent with measurements on polycrystalline samples of the same compound [68]. Hence, the intrinsic electrical transport properties of the $LnO_{1−x}F_xBiS_2$ compounds seem to be dependent on a combination of lanthanide element Ln, F concentration x, and quality of the samples.
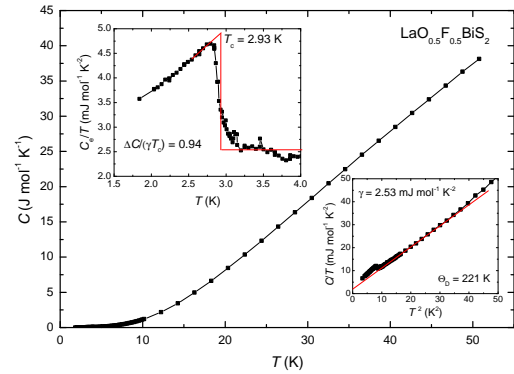
Both zero-field-cooled (ZFC) and field-cooled (FC) measurements of $\chi(T)$ were performed for $LnO_{1−x}F_xBiS_2$ samples with different Ln and F concentrations. As shown in Fig. 8, ZFC measurements on $LnO_{0.5}F_{0.5}BiS_2$ ($Ln =$ La, Pr, Nd) yield a significant shielding volume fraction with T_c onset values that are consistent with the $\rho(T)$ data, while FC measurements reveal that $\chi(T)$ remains nearly unchanged in the superconducting state relative to the normal state, indicating strong vortex pinning [21]. For the case of samples with $Ln =$ Ce and Yb and nominal F concentrations of $x \geqslant 0.7$ and $x = 0.5$, respectively, magnetic phase transitions were also observed, apart from diamagnetic signals arising from the appearance of superconduc-
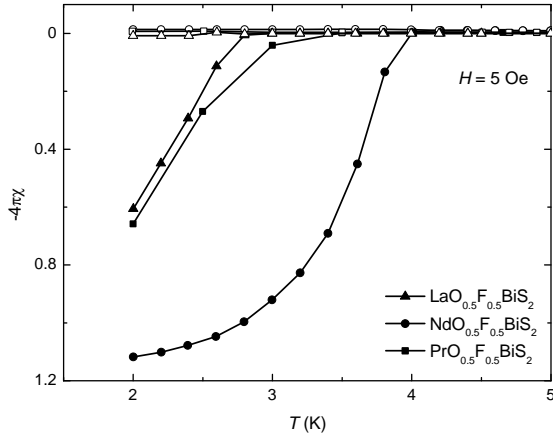
Figure 8: Temperature dependence of the magnetic susceptibility χ for $Ln\mathrm{O}_{0.5}\mathrm{F}_{0.5}\mathrm{BiS}_2$ (*Ln* = La, Pr, Nd) measured in the field-cooled (FC) (open symbols) and zero-field-cooled (ZFC) (filled symbols) processes. The data are taken from Ref. [21].

Figure 9: (Color online) Specific heat C vs temperature T for $\mathrm{LaO}_{0.5}\mathrm{F}_{0.5}\mathrm{BiS}_2$. A plot of C/T vs T^2 is shown in the inset in the lower right hand part of the figure. The red line is a fit of the expression $C(T)/T = \gamma + \beta T^2$. A plot of C_e/T vs T, where C_e is the electronic contribution to the specific heat, in the vicinity of the superconducting transition is shown in the inset in the upper left hand side of the figure. The data are taken from Ref. [21].

tivity [21, 70, 72]. In addition to the induction of superconductivity and enhancement of T_c as a result of F substitution, the shielding volume fraction may be significantly enhanced at those temperatures where it has begun to saturate as a result of the increase in F concentration; a typical example of this behavior was found for $\mathrm{NdO}_{1-x}\mathrm{F}_x\mathrm{BiS}_2$ reported in Ref. [47].

Figure 9 displays specific heat $C(T)$ data for the polycrystalline $\mathrm{LaO}_{0.5}\mathrm{F}_{0.5}\mathrm{BiS}_2$ compound in the temperature range 1.8 K $\leqslant T \leqslant$ 50 K [21]. The expression $C(T)/T = \gamma + \beta T^2$, where γ is the electronic specific heat coefficient and β is the coefficient of the lattice contribution, was used to fit the C/T vs T^2 data in the normal state which is displayed in the inset in the lower right hand side of Fig. 9. Shown in the inset in the upper left hand side of Fig. 9 are C_e/T vs T data, where C_e is the electronic contribution to the specific heat. Bulk superconductivity in polycyrstalline $\mathrm{LaO}_{0.5}\mathrm{F}_{0.5}\mathrm{BiS}_2$ was confirmed with the appearance of a clear jump in the C_e/T vs T data at T_c. The ratio of the observed jump to the electronic contribution to the specific heat at T_c is estimated to be $\Delta C/\gamma T_c$ = 0.94, which is lower than the weak coupling BCS value of 1.43, but large enough to confirm bulk superconductivity in this compound. For the other $Ln\mathrm{O}_{0.5}\mathrm{F}_{0.5}\mathrm{BiS}_2$ compounds with Ln = Ce, Pr, Nd, and Yb, the significant upturns in the C/T vs T data observed at low temperature are likely due to the presence of a Schottky-like anomaly for Ln = Pr and Nd or magnetic ordering for Ln = Ce and Yb [21, 74]. No clear $C(T)/T$ jump related to the appearance of superconductivity was observed in these samples [21]. The jumps in $C(T)/T$ in these compounds may not be readily observable because they may be reduced by the pairbreaking interac-

tion due to the magnetic ions; the jumps may also be obscured by the broadening of the superconducting transitions by sample inhomogeneity or by the large upturns in $C(T)/T$. More rigorous experimental and theoretical studies on higher quality samples are needed to establish the nature of superconductivity in these compounds.

4 $\mathrm{La}_{1-x}M_x\mathrm{OBiS}_2$ (*M* = Th, Hf, Zr, and Ti)
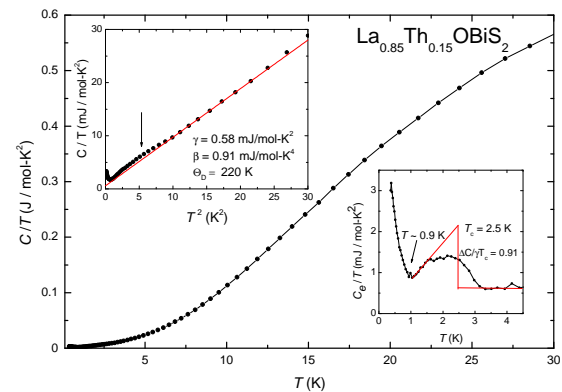
As an alternative to F substitution, electron doping in the LaOBiS_2 system is possible by partially replacing trivalent La with tetravalent M (*M* = Th, Hf, Zr, and Ti) [25]. It has been reported that the $\mathrm{La}_{1-x}M_x\mathrm{OBiS}_2$ system exhibits superconductivity with values of T_c up to 2.85 K. A comparison of T_c values observed in the various compounds is displayed in the inset of Fig. 10 in which 20% ($x = 0.2$) of M = Th, Hf, Zr, and Ti was substituted for La in $\mathrm{La}_{1-x}M_x\mathrm{OBiS}_2$; there appears to be no clear correlation between T_c and the ionic radius of the tetravalent ion that replaces the La ion. The lowest value of T_c is observed for the $\mathrm{La}_{0.8}\mathrm{Zr}_{0.2}\mathrm{OBiS}_2$ compound; while sharper superconducting transitions are observed for the $\mathrm{La}_{0.8}\mathrm{Hf}_{0.2}\mathrm{OBiS}_2$ and $\mathrm{La}_{0.8}\mathrm{Ti}_{0.2}\mathrm{OBiS}_2$ compounds, broader transitions are observed for the $\mathrm{La}_{0.8}\mathrm{Zr}_{0.2}\mathrm{OBiS}_2$ and $\mathrm{La}_{0.8}\mathrm{Th}_{0.2}\mathrm{OBiS}_2$ compounds. X-ray diffraction experiments show that both the a and c lattice parameters do not change significantly with different M^{4+} substitutions at the $x = 0.2$ concentration.
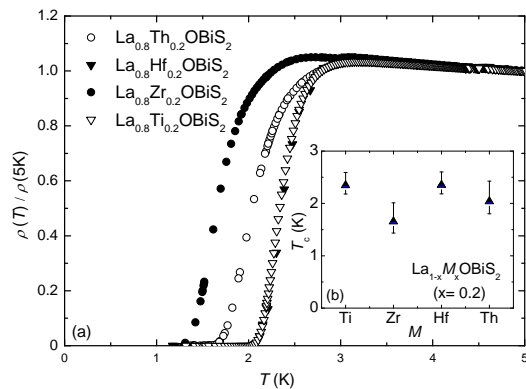
Figure 10: Resistive superconducting transitions and (inset) superconducting transition temperatures T_c for $La_{1-x}M_xOBiS_2$ compounds with M = Th, Hf, Zr, Ti and x = 0.2. T_c is defined as the temperature where resistivity drops to 50% of its normal state value, and the width of the transition is determined from the temperatures where the resistivity drops to 90% and 10% of its normal state value. Reprinted with permission from Ref. [25]. Copyright (2013) by the American Physical Society.

Figure 11: (Color online) Specific heat C divided by temperature T, C/T, vs T for $La_{0.85}Th_{0.15}OBiS_2$. C/T vs T^2 is shown in the inset in the upper left hand part of the figure. The red line is a fit of the expression $C(T)/T = \gamma + \beta T^2$ to the data. The inset in the lower right part of the figure shows a plot of $C_e(T)$ vs T in the vicinity of the superconducting transition. Reprinted with permission from Ref. [25]. Copyright (2013) by the American Physical Society.

However, with increasing M concentration, both values of a and c for $La_{1-x}M_xOBiS_2$ were observed to decrease gradually. For $La_{1-x}Th_xOBiS_2$, T_c first decreases with x from 2.85 K at x = 0.15 to 2.05 K at x = 0.20 and then remains roughly constant at higher concentration. A similar evolution of T_c with increasing M was also observed for $La_{1-x}M_xOBiS_2$ (M = Hf, Ti); however, after partially replacing La^{3+} with Sr^{2+}, no superconductivity was observed in $La_{1-x}Sr_xOBiS_2$ down to ~1 K in the range $0.1 \leqslant x \leqslant 0.3$, which is in agreement with the behavior reported for $La_{1-x}Mg_xOBiS_2$ (x = 0 to 0.2) samples [25, 75]. These results suggest that hole doping is not sufficient to induce superconductivity and reveal the importance of electron doping in achieving superconductivity in BiS_2-based compounds.

Measurements of $\rho(T)$ for the $La_{0.85}Th_{0.15}OBiS_2$ and $La_{0.8}Hf_{0.2}OBiS_2$ compounds were performed in various magnetic fields down to 0.36 K [25]. As magnetic field is increased, the superconducting transition width broadens and the onset of superconductivity gradually shifts to lower temperatures. The orbital critical fields $H_{c2}(0)$ for the $La_{0.85}Th_{0.15}OBiS_2$ and $La_{0.8}Hf_{0.2}OBiS_2$ compounds were inferred from their initial slopes of H_c with respect to T using the conventional one-band WHH theory [39], yielding values of 1.09 and 1.12 T, respectively. These values of $H_{c2}(0)$ are close to the values of 1.9 T for $H_{c2}(0)$ observed in $LaO_{0.5}F_{0.5}BiS_2$ [18, 21], suggesting that there is a common superconducting phase characteristic of BiS_2-based superconductors.

Specific heat measurements were performed for the $La_{0.85}Th_{0.15}OBiS_2$ and $La_{0.8}Hf_{0.2}OBiS_2$ compounds in the temperature range of $0.36\,K \leqslant T \leqslant 30\,K$ [25]. A clear feature was observed between 1 and 3 K for $La_{0.85}Th_{0.15}OBiS_2$ as shown in the inset at the lower right hand side of Fig. 11. A value of T_c = 2.5 K was estimated from an idealized entropy conserving construction, which is close to the T_c obtained from $\rho(T)$ measurement (T_c = 2.85 K). The presence of the feature suggests that superconductivity is a bulk phenomenon in this compound. The value of $\Delta C/\gamma T_c$ for $La_{0.85}Th_{0.15}OBiS_2$ is estimated to be ~0.91, which is less than the value of 1.43 predicted by the BCS theory, but similar to that seen in $LaO_{0.5}F_{0.5}BiS_2$ [21]. However, only a small feature in the C_e/T data for $La_{0.8}Hf_{0.2}OBiS_2$ is observed around the value of T_c (2.36 K) obtained from $\rho(T)$ measurements. The absence of a well-defined superconducting jump at T_c for $La_{0.8}Hf_{0.2}OBiS_2$ is likely to be a consequence of the superconducting transition being spread out in temperature due to sample inhomogeneity [21].

5 Chemical substitution effects on Ln(O,F)BiS$_2$

It has been demonstrated that the charge carrier (electron) density is important for the superconductivity of BiS_2-based compounds. In addition, values of T_c for AG samples of $LnO_{0.5}F_{0.5}BiS_2$ increase with increasing atomic number of the Ln component as shown in Fig. 6 [21, 22].
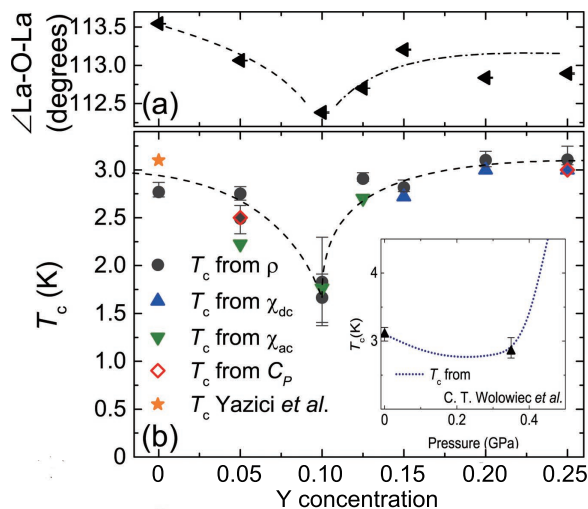
Figure 12: (Color online) (a) La(Y)-O(F)-La(Y) bond angle vs nominal yttrium concentration. (b) Dependence of T_c on Y concentration for the La$_{1-x}$Y$_x$O$_{0.5}$F$_{0.5}$BiS$_2$ system. The orange star is the T_c of LaO$_{0.5}$F$_{0.5}$BiS$_2$ reported in Ref. [21]. The inset shows the behavior of T_c under hydrostatic pressure [30]. Reprinted with permission from Ref. [42]. Copyright (2014) by the American Physical Society.

(The ionic size of the Ln^{3+} ion decreases with increasing atomic number.) This size contraction has the effect of reducing the dimensions of the blocking layers which contain the Ln^{3+} ions, thereby squeezing the neighboring BiS$_2$ layers, i.e., effectively generating chemical pressure on the superconducting BiS$_2$ layers. As discussed in section 3.1, it appears that there is a correlation between T_c and the decrease in the size of the a-axis in the Ln(O,F)BiS$_2$ system. Hence, substitution of the element La with heavier lanthanide elements such as Sm, Eu, and Gd holds promise as a strategy for further enhancement of T_c in the BiS$_2$-based superconducting compounds. Recently, the compound with nominal chemical composition SmO$_{0.5}$F$_{0.5}$BiS$_2$ was synthesized and reported to be non-superconducting [76]; attempts have been unsuccessful in synthesizing other LnO$_{0.5}$F$_{0.5}$BiS$_2$ compounds with Ln = Eu-Tm. However, there has been recent success in synthesizing compounds in which there is a partial substitution at the Ln site with relatively smaller atoms as a method for enhancing T_c and further determining which parameters are relevant in affecting superconductivity [41, 42, 75–79].

As an example, partial substitution of La with the smaller Y ions in the La$_{1-x}$Y$_x$O$_{0.5}$F$_{0.5}$BiS$_2$ compound allows one to study the effects of chemical pressure on superconductivity [42]. Similar to La, Y has a trivalent electronic configuration and no magnetic moment, making Y^{3+} a suitable replacement for the La^{3+} ions. As a result of the substitution of Y for La in La$_{1-x}$Y$_x$O$_{0.5}$F$_{0.5}$BiS$_2$, T_c was found to gradually decrease from 2.8 K at $x = 0$ to
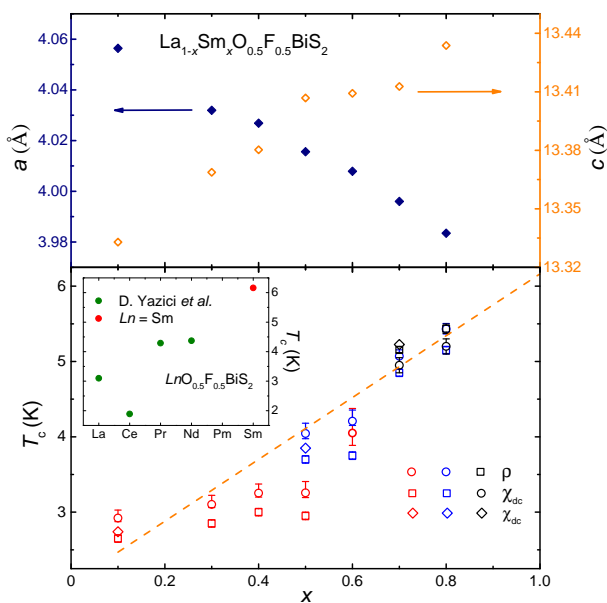
Figure 13: (Color online) Dependence of the lattice constants a and c (upper panel) and T_c (lower panel) on Sm concentration x of La$_{1-x}$Sm$_x$O$_{0.5}$F$_{0.5}$BiS$_2$. Red, blue, and purple symbols in the lower panel represent results for samples annealed at 800°C, 750°C, and 710°C, respectively. The inset shows representative values of T_c of Ln(O,F)BiS$_2$ reported in Ref. [21]. The other data are obtained from Ref. [41].

1.8 K at $x = 0.1$ and then remain roughly constant at ∼3.0 K for $x \geqslant 0.125$ as shown in Fig. 12. The lattice parameter a and the unit cell volume of La$_{1-x}$Y$_x$O$_{0.5}$F$_{0.5}$BiS$_2$ monotonically decrease with increasing Y concentration until the solubility limit $x = 0.20$. Interestingly, the evolution of the La-O-La bond angle with increasing x closely follows the evolution of $T_c(x)$ as shown in Fig. 12. It should be mentioned that the lattice constant c changes in the opposite manner (decreasing with increasing Y concentration), which suggests that T_c may also be affected by the value of c. Unfortunately, due to the solubility limit of Y in La$_{1-x}$Y$_x$O$_{0.5}$F$_{0.5}$BiS$_2$, further investigation of the relation between lattice parameters, bond angle, and T_c by the method of substitution is not possible and the highest chemical pressure obtained in La$_{0.8}$Y$_{0.2}$O$_{0.5}$F$_{0.5}$BiS$_2$ is still lower than 0.7 GPa, above which a structural phase transition from tetragonal ($P4/nmm$) to monoclinic ($P21/m$) has been observed in LaO$_{0.5}$F$_{0.5}$BiS$_2$ under applied external hydrostatic pressure [30, 80].

Figure 13 shows the Sm concentration dependence of T_c for La$_{1-x}$Sm$_x$O$_{0.5}$F$_{0.5}$BiS$_2$. An enhancement of superconductivity is observed in the La$_{1-x}$Sm$_x$O$_{0.5}$F$_{0.5}$BiS$_2$ compound in which T_c increases from ∼2.8 K at $x = 0.1$ to 5.4 K at the solubility limit of $x = 0.8$ [41]. A linear extrapolation of the $T_c(x)$ data beyond the $x = 0.8$ solubility

limit to $x = 1.0$ allows for an estimate of the value of T_c for the parent compound $SmO_{0.5}F_{0.5}BiS_2$ to be as high as ~ 6.2 K; this value of T_c is significantly higher than values of T_c reported for other AG samples of the $LnO_{0.5}F_{0.5}BiS_2$ compound and is therefore consistent with the trend that higher values of T_c are observed in $LnO_{0.5}F_{0.5}BiS_2$ compounds containing a Ln element having a larger atomic number (see the inset of Fig. 13). As the Sm concentration increases from $x = 0.1$ to 0.8, the lattice constant c increases while the lattice constant a gradually decreases, resulting in an overall suppression of the unit cell volume of $\sim 3\%$, however, no structural phase transition is observed. In comparison, there is approximately only a $\sim 2\%$ decrease in the unit cell volume of $LaO_{0.5}F_{0.5}BiS_2$ before the pressure-induced structure phase transition [80]. Hence, the effects of Sm substitution for La and applied hydrostatic pressure on the compound $LaO_{0.5}F_{0.5}BiS_2$ seem somewhat different.

Effects of substitutions at the Ln site in the $LnO_{0}.5F_{0}.5BiS_2$ compounds were also investigated at various F concentrations which allows for the study of the tuning of the lattice constant c and its effects on superconductivity. Phase diagrams of T_c vs Ln substitution for the $Ce_{1-x}Nd_xO_{1-y}F_yBiS_2$ and $Nd_{1-z}Sm_zO_{1-y}F_yBiS_2$ systems were determined from measurements of magnetization at nominal F concentrations of $y = 0.7$, 0.5, and 0.3 as shown in Fig. 14 [78]. Superconductivity is induced and noticeably enhanced for those compounds containing higher concentrations of Ln elements with relatively smaller atomic size (or larger atomic number), i.e., higher concentrations of Nd and Sm atoms. The shift in the phase boundary to the right for decreasing F concentration suggests the importance of F concentration in the induction of superconductivity in these BiS_2-based compounds. For a given F concentration, it appears that superconductivity is enhanced in compounds with Ln ions of smaller ionic size; however, there is no appreciable increase in T_c for greater concentrations of F. It is interesting to note that samples with different nominal values of F concentration that share similar values of T_c also exhibit similar values of the ratio of the length of the c-axis to that of the a-axis (see Fig. 14(b)); this implies that the superconductivity observed in the BiS_2-based compounds is closely related with the lattice constant ratio c/a. The effect of charge carrier density on the enhancement of superconductivity in these BiS_2-based compounds seems to be of less importance in comparison to the lattice parameter a and the c/a ratio.

The role of the charge carrier density in the enhancement of superconductivity is emphasized in the study of the $La_{1-x}Mg_xO_{1-2x}F_{2x}BiS_2$ system in which Mg^{2+} and F^-
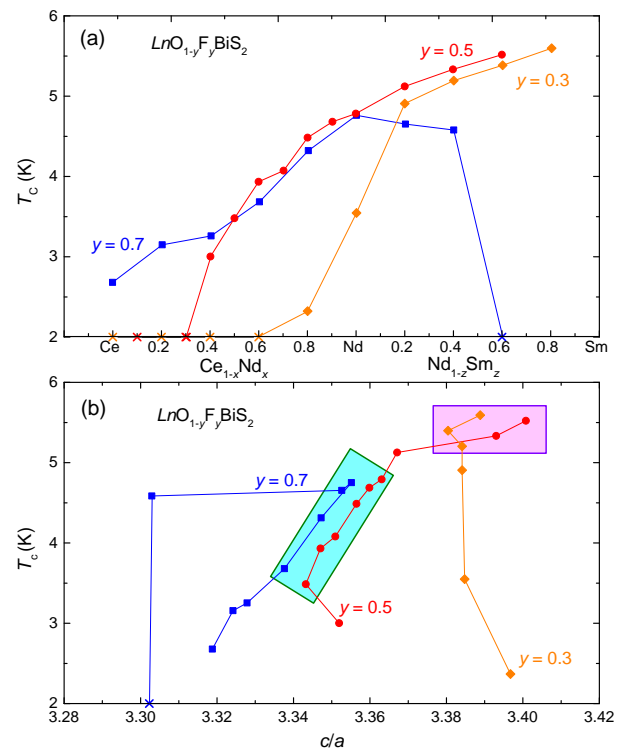
Figure 14: (Color online) (Color online) Superconducting critical temperature T_c of $LnO_{1-y}F_yBiS_2$ ($y = 0.7$, 0.5, and 0.3) as a function of Ln concentration. The cross symbols indicate that a superconducting transition is not observed above 2 K. Reprinted with permission from Ref. [78] J. Kajitani, T. Hiroi, A. Omachi, O. Miura, Y. Mizuguchi, J. Phys. Soc. Jpn. **84** (2015) 044712. Copyrighted by the Physical Society of Japan.

are substituted for La^{3+} and O^{2-}, respectively [75]. Superconductivity is observed for nominal $x \geqslant 0.2$ where T_c continues to increase up to ~ 3 K at $x = 0.3$, which is slightly beyond the solubility limit of $x = 0.25$. For a fixed F concentration at $2x = 0.4$, the introduction of Mg^{2+} ions into the $LaO_{0.6}F_{0.4}BiS_2$ compound generates holes in the BiS_2 superconducting layers which have the effect of suppressing superconductivity and thereby reducing T_c despite the reduction in lattice parameters. The research also indicates that a reduction in lattice parameters leads to an enhancement of T_c. For instance, a reduction in the values of the lattice parameters appears to enhance superconductivity when comparing the $La_{0.8}Ca_{0.2}O_{0.6}F_{0.4}BiS_2$ and $La_{0.8}Mg_{0.2}O_{0.6}F_{0.4}BiS_2$ compounds which have T_c values of 2.07 K and 2.54 K, respectively.

6 Superconductivity of $LnO_{0.5}F_{0.5}BiS_2$ under applied pressure

In addition to chemical substitution, the application of external pressure is another means to induce fundamental change to both the crystalline and electronic structure which can have a significant impact on the superconducting properties of the layered BiS$_2$-based compounds. The first report of a dramatic and abrupt increase in T_c from $\sim$3 to 10.7 K for the LaO$_{0.5}$F$_{0.5}$BiS$_2$ compound under pressure is shown in the upper panel of Fig. 15(a). In the $T_c(P)$ phase diagram, there is an obvious transition from a low-T_c superconducting phase to a high-T_c superconducting phase [30]. The phenomenon was soon reported to be associated with a pressure-induced first order phase transition from a tetragonal to a monoclinic crystal structure in which there is a relative shift, or sliding, of the two neighboring BiS$_2$ layers along the a-axis [80]. Similar behavior in the evolution of T_c with pressure has also been observed in other $LnO_{0.5}F_{0.5}BiS_2$ (Ln = Ce, Pr, Nd) compounds as shown in the $T_c(P)$ phase diagrams of Fig. 16 [29].
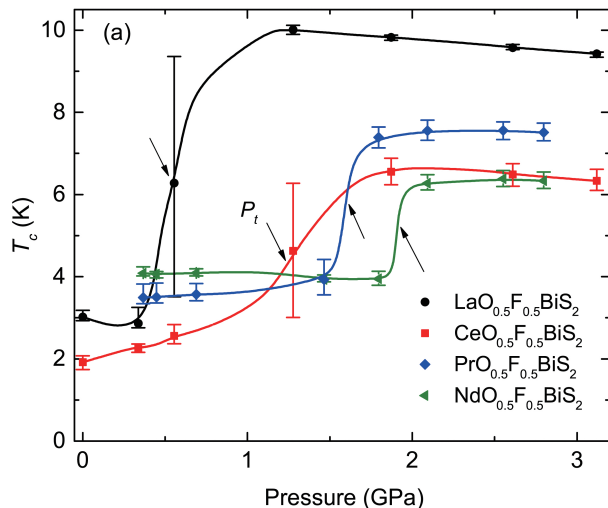
Interestingly, the critical transition pressure, P_t, that marks the low-T_c to high-T_c phase transition in the superconducting state is coincident with changes in the normal state electrical transport properties in the $LnO_{0.5}F_{0.5}BiS_2$ system; the pressure-induced phase transition corresponds with a saturation in the rate of suppression of semiconducting-like behavior in the normal state [30]. In the case of the NdO$_{0.5}$F$_{0.5}$BiS$_2$ compound, a semiconductor-metal transition occurs at P_t as shown in Fig. 15(b) [29]. Such changes in the behavior of the normal state electrical resistivity, $\rho(T)$, indicate that there may be increases in the density of charge carriers that correspond to the rapid increase in T_c.

AG samples from the series of $LnO_{0.5}F_{0.5}BiS_2$ compounds with Ln elements of smaller atomic radius (i.e., larger atomic number) exhibit higher T_c values when compared with compounds containing Ln elements of larger atomic radius suggesting that T_c correlates with the lattice parameters. Given the correlation between T_c and the lattice parameters, one might expect that the pressure-induced phase transitions observed for the various $LnO_{0.5}F_{0.5}BiS_2$ compounds would occur at a characteristic and consistent value of the lattice parameter a across the $LnO_{0.5}F_{0.5}BiS_2$ series. Furthermore, considering the results from substitution studies discussed earlier in this article, one would expect a smaller applied pressure to induce the phase transition for those
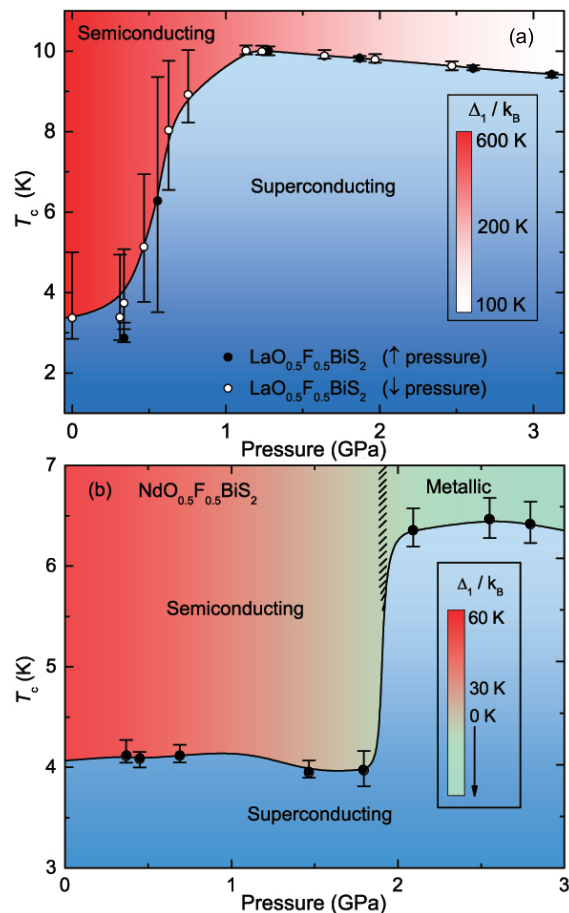
Figure 15: (Color online) $T_c(P)$ phase diagrams for (a) LaO$_{0.5}$F$_{0.5}$BiS$_2$ and (b) NdO$_{0.5}$F$_{0.5}$BiS$_2$. The red color gradient represents the suppression of the semiconducting behavior with pressure as manifested in the decrease of the semiconducting energy gap Δ_1/k_B whose values are indicated in the legend. The green region to the right of the crosshatching in (b) corresponds to the metallization of NdO$_{0.5}$F$_{0.5}$BiS$_2$. (a), (b) Reprinted with permission from Ref. [30] (copyright (2013) American Physical Society) and Ref. [29] (Enhancement of superconductivity near the pressure-induced semiconductor-metal transition in the BiS$_2$-based superconductors $LnO_{0.5}F_{0.5}BiS_2$ (Ln = La, Ce, Pr, Nd), J. Phys.: Condens. Matter 25 (2013) 422201. Copyright (2013) by the IOP Publishing.), respectively. For interpretation of the definition of T_c, vertical bars, and Δ_1/k_B, the reader is referred to the web versions of the corresponding articles.

$LnO_{0.5}F_{0.5}BiS_2$ compounds with Ln elements exhibiting smaller values of the lattice parameter a. To the contrary, the a-axis lattice parameters at P_t are not constant across the series $LnO_{0.5}F_{0.5}BiS_2$. The lattice parameter a for the LaO$_{0.5}$F$_{0.5}$BiS$_2$ compound just before the transition pressure, $P_t \sim$ 0.7 GPa, is estimated to be 4.08 Å which is larger than the values of a for other members of the $LnO_{0.5}F_{0.5}BiS_2$ series at ambient pressure [21, 80]. The $T_c(P)$ phase diagrams depicted in Fig. 16 indicate that the

Figure 16: (Color online) Pressure dependence of T_c for $LnO_{0.5}F_{0.5}BiS_2$ (Ln = La, Ce, Pr, Nd). The black arrows indicate the critical transition pressures from the low-T_c to high-T_c superconducting phases. Reprinted with permission from Ref. [29]: Enhancement of superconductivity near the pressure-induced semiconductor-metal transition in the BiS$_2$-based superconductors $LnO_{0.5}F_{0.5}BiS_2$ (Ln = La, Ce, Pr, Nd), J. Phys.: Condens. Matter 25 (2013) 422201. Copyright (2013) by the IOP Publishing.

critical transition pressure P_t increases as the atomic size of the Ln ions decreases and that the jump in T_c during the phase transition (ΔT_c) is smaller for smaller Ln ions in $LnO_{0.5}F_{0.5}BiS_2$ [29, 30]. Heavier Ln ions seem to help stabilize the structure of the $LnO_{0.5}F_{0.5}BiS_2$ against external pressure.

Figure 17 shows the evolution of T_c for the $La_{1-x}Sm_xO_{0.5}F_{0.5}BiS_2$ compound as a function of both pressure and Sm concentration x [81]. Similar to the $LnO_{0.5}F_{0.5}BiS_2$ compounds, the $La_{1-x}Sm_xO_{0.5}F_{0.5}BiS_2$ system exhibits a reversible pressure-induced transition from a low-T_c (SC1) to a high-T_c (SC2) superconducting phase. It has been shown that the lattice parameter a in the $La_{1-x}Sm_xO_{0.5}F_{0.5}BiS_2$ compound is significantly reduced by increasing the Sm concentration x [41]. The results for the SC1 to SC2 phase transition in the $La_{1-x}Sm_xO_{0.5}F_{0.5}BiS_2$ system indicate that optimization of T_c could be achieved in $La_{1-x}Sm_xO_{0.5}F_{0.5}BiS_2$ by decreasing the a lattice parameter (high Sm concentration) in the SC1 phase at ambient pressure or by increasing a (low Sm concentration) in the SC2 phase under pressure.

Although the chemical composition of the blocking layers in the $LnO_{0.5}F_{0.5}BiS_2$ and $La_{1-x}Sm_xO_{0.5}F_{0.5}BiS_2$ compounds are different, their evolution of T_c with pressure is similar. As displayed in Fig. 18(a), P_t increases with decreasing atomic size of the Ln ion for $LnO_{0.5}F_{0.5}BiS_2$ (Ln = La, Ce, Pr, Nd) compounds in the same way
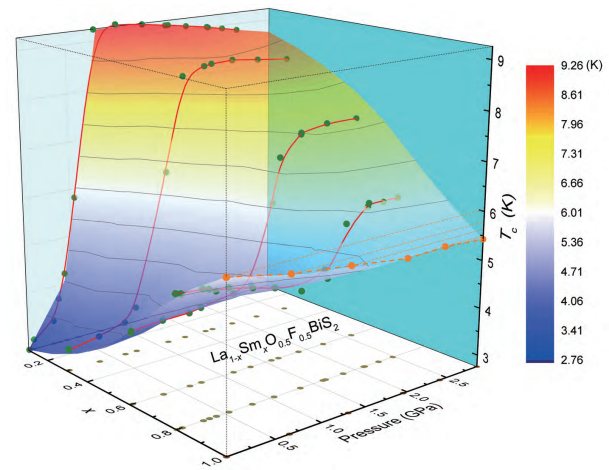

Figure 17: (Color online) Superconducting critical temperature T_c of $La_{1-x}Sm_xO_{0.5}F_{0.5}BiS_2$ (x = 0.1-0.8) plotted as a function of pressure and nominal Sm concentration x. Filled circles in the x-y plane are projections of T_c. The data are taken from Ref. [81]. (For interpretation of the estimated T_c values of $SmO_{0.5}F_{0.5}BiS_2$, the reader is referred to Ref. [81].)

that P_t increases with increasing Sm concentration for $La_{1-x}Sm_xO_{0.5}F_{0.5}BiS_2$ under pressure [29, 81]. If we plot ΔT_c for $LnO_{0.5}F_{0.5}BiS_2$ and $La_{1-x}Sm_xO_{0.5}F_{0.5}BiS_2$ as a function of lattice parameter a, they follow the same linear trend, despite the differences in the chemical composition of their blocking layer. This suggests the importance of the in-plane separation between ions in the superconducting BiS$_2$ layers and its effect on superconductivity in the BiS$_2$-based compounds under pressure. However, there is no clear relationship observed between the c lattice parameter and superconductivity in these BiS$_2$-based compounds under pressure.

Partial substitution of Ln ions with smaller ions typically results in a reduction of the a lattice parameter and along with (but not always) a slight increase in the c lattice parameter; however, it has been reported that both the a and c lattice parameters can be simultaneously suppressed with the application of hydrostatic pressure [80]. This has implications for the behavior of superconductivity under external pressure as being fundamentally different when compared to the behavior of superconductivity in response to chemical substitution in the BiS$_2$-based compounds. As an example, it was reported that a structural phase transition from the tetragonal phase to the monoclinic phase occurs at ~0.7 GPa in $LaO_{0.5}F_{0.5}BiS_2$ under pressure, whereas it is known that all BiS$_2$-based superconductors at ambient pressure exhibit the tetragonal phase, including those compounds subject to heavy chemical substitution. As another example, the T_c of AG samples of $LaO_{0.5}F_{0.5}BiS_2$ increases with a reduction in the
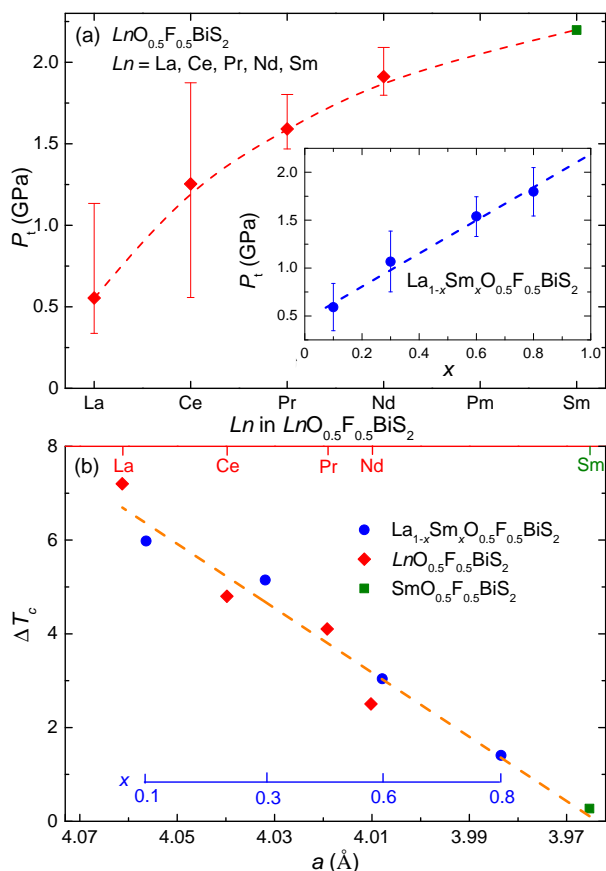
Figure 18: (Color online) (a) Evolution of P_t as a function of Ln in $LnO_{0.5}F_{0.5}BiS_2$. The inset in panel (a) shows Sm concentration dependence of P_t for $La_{1-x}Sm_xO_{0.5}F_{0.5}BiS_2$. (b) ΔT_c vs lattice parameter a of $La_{1-x}Sm_xO_{0.5}F_{0.5}BiS_2$ and $LnO_{0.5}F_{0.5}BiS_2$. Dashed lines are guides to the eye. ΔT_c and P_t values of $LnO_{0.5}F_{0.5}BiS_2$ and $La_{1-x}Sm_xO_{0.5}F_{0.5}BiS_2$ are taken from Refs. [29] and [81], respectively. The values of the lattice parameter a for $LnO_{0.5}F_{0.5}BiS_2$ and $La_{1-x}Sm_xO_{0.5}F_{0.5}BiS_2$ are obtained from Refs. [74] and [41], respectively. (For interpretation of the estimated data of $SmO_{0.5}F_{0.5}BiS_2$, the reader is referred to Refs. [41, 81].)

lattice parameter a through a partial or full replacement of La with heavier (smaller) Ln, whereas further reduction of the lattice parameter a by increasing external hydrostatic pressure up to 1.5 GPa results in a gradual decrease in T_c of $La_{0.2}Sm_{0.8}O_{0.5}F_{0.5}BiS_2$ [81]. Rather than adopting a single lattice parameter determination in explaining the effects of applied pressure on superconductivity in these BiS_2-based compounds, these observations suggest that there is a complex interplay of various parameters and their effects on superconductivity under pressure. In addition to the importance of the size of the lattice constant a in affecting superconductivity, reduction of the lattice constant c also appears to affect the superconducting state of BiS_2-based compounds. By applying uniaxial pressure along the c-axis in single crystalline $PrO_{0.5}F_{0.5}BiS_2$, a low-T_c to high-

T_c phase transition is also observed at 0.7 GPa, which is significantly lower than the P_t of $PrO_{0.5}F_{0.5}BiS_2$ under hydrostatic pressure [82]. Until now, although a large number of compounds in the BiS_2 family have been investigated in terms of their transport behavior under pressure, reports on the evolution of crystal structure with pressure are very limited. To clarify correlations between the crystal structure of BiS_2-based compounds and their superconductivity under pressure, further experiments involving the use of in-situ x-ray diffraction/absorption measurements under pressure need to be performed on different BiS_2-based samples in both polycrystal and single crystal form.

7 Se-substituted $LnO_{0.5}F_{0.5}BiS_2$

Most of the research regarding chemical substitution and superconductivity in the Ln(O,F)BiS_2 compounds has been devoted to studying the effects of elemental substitution in the blocking LnO layers. There has been much less effort and only a few reports regarding the effects on superconductivity that result from modification of the superconducting BiS_2 layers. Substitution of Sb for Bi appears to be an ineffective means for enhancing superconductivity. While $LaO_{0.5}F_{0.5}BiS_2$ has a $T_c \sim 3$ K, $LaO_{0.5}F_{0.5}SbS_2$ does not exhibit superconductivity above 1.7 K [83]. Furthermore, it appears that a small amount of Sb substitution (10%) in the $NdO_{0.5}F_{0.5}BiS_2$ compound strongly suppresses superconductivity [84]. Alternatively, it is possible to completely replace S with either Se or Te in $LaO_{0.5}F_{0.5}BiS_2$; however, only the $LaO_{0.5}F_{0.5}BiSe_2$ compound was found to exhibit superconductivity with a $T_c \sim 2.6$ K [83]. The Se^{2-} and S^{2-} ions are chemically similar; however, the Se^{2-} ionic radius of 1.98 Å is larger than the S^{2-} ionic radius of 1.84 Å (assuming a coordination number of 6) [79]. This distinction may prove useful in studies on the effects of Se substitution in the $LnO_{0.5}F_{0.5}BiS_2$ system from which new insights and perspectives might be gained regarding the relationship between crystal structure and superconductivity in the Ln(O,F)BiS_2 compounds.

The dependence of T_c on the concentration of Se, substituted for S in $LnO_{0.5}F_{0.5}BiS_2$, exhibits complicated behavior when the Ln element changes. For polycrystalline $NdO_{0.5}F_{0.5}Bi(S_{1-x}Se_x)_2$ ($x \leqslant 0.2$), it has been reported that, as the Se concentration is increased, there is a noticeable change in the lattice constant a, but no significant change in the lattice constant c; in addition, both T_c and the shielding volume fraction of $NdO_{0.5}F_{0.5}Bi(S_{1-x}Se_x)_2$ decrease with increasing Se concentration [84]. These re-
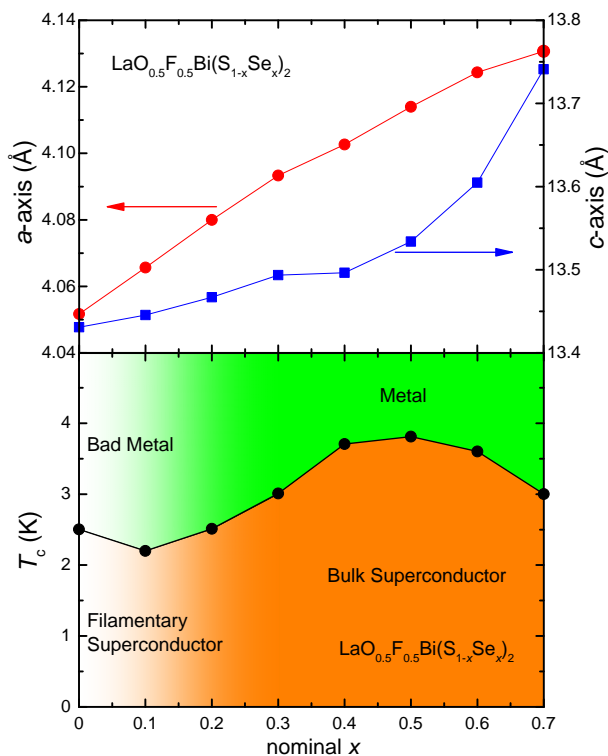
Figure 19: (Color online) Nominal Se concentration dependence of lattice constants a and c (upper) and T_c (lower). Reprinted with permission from Ref. [85] T. Hiroi, J. Kajitani, A. Omachi, O. Miura, Y. Mizuguchi, J. Phys. Soc. Jpn. 84 (2015) 024723. Copyrighted by the Physical Society of Japan.

sults are consistent with the previous discussion regarding modification of the LnO blocking layers in which superconductivity is enhanced as the lattice parameters are reduced. In the case of $LaO_{0.5}F_{0.5}Bi(S_{1-x}Se_x)_2$, T_c increases from 2.4 K at $x = 0.2$ to 3.8 K at $x = 0.5$ with a large shielding volume fraction followed by a slight decrease in T_c for $x > 0.5$ [79, 85]. Synchrotron X-ray diffraction experiments performed on the $LaO_{0.5}F_{0.5}Bi(S_{1-x}Se_x)_2$ compound show that Se atoms are more likely to occupy in-plane S1 sites rather than the out-of-plane S2 sites, resulting in an expansion in both the a and c axes with increasing Se concentration [79]. This behavior complicates the picture we have regarding the correlation between the crystal structure and superconductivity in the BiS_2-based compounds.

8 Concluding remarks

There is already a significant amount of interesting behavior reported on the effects of chemical substitution in the recently discovered family of BiS_2-based compounds; and many of these interesting properties are often not exhib-

ited in the parent form of these compounds. The LnBiOS$_2$ compounds were synthesized and reported as early as 1995 [86]; however, no superconductivity was found in the LnBiOS$_2$ system until electron doping studies were performed in 2012 [10, 19–21]. Hence, the introduction of charge carriers (electrons) into the parent compound is regarded to be essential for the emergence of superconductivity in BiS_2-based superconductors [20, 74]. Measurements of $\rho(T)$ under pressure provide supporting evidence that the dramatic enhancement of superconductivity in various $LnO_{0.5}F_{0.5}BiS_2$ compounds is coincident with an increase in the charge carrier density [29, 30].

Substitution for ions in either the BiS_2 superconducting layers or the blocking LnO layers with ions of different atomic size allows one to tune the lattice parameters as well as the local lattice structure of the BiS_2-based compounds and thereby generate chemical pressure. An increase in chemical pressure in the superconducting BiS_2 layers would result in a shorter Bi-S1 bond distance thereby enhancing the overlap of the Bi-6p and S-p orbitals; this would allow superconductivity to be tuned without a dramatic change of charge carrier density. Experimental evidence suggests that both the contraction along the a-axis and the c/a ratio play an essential role in the emergence of superconductivity in some LnBi(O,F)S$_2$ compounds [21, 41, 75, 77, 78]. However, the clear correlation between lattice contraction and superconductivity does not apply to all BiS_2-based compounds and fails to hold when samples are subjected to hydrostatic pressure. At present, finding a universal relationship between the crystal structure and superconductivity in the BiS_2-based compounds is still one of the main challenges in this research area. Recently, Mizuguchi *et al.* defined a value of in-plane chemical pressure as $(R_{Bi} + R_{S1})$/Bi-S1(in-plane), where R_{Bi} is the estimated ionic radius of $Bi^{2.5+}$, R_{S1} is the estimated average ionic radius of the chalcogen at the S1 site, and the Bi-S1 bond distance is obtained from the Rietveld refinement of experimental XRD data [79]. A clear correlation between T_c and the in-plane chemical pressure is observed in the $LnO_{0.5}F_{0.5}BiS_2$ (Ln = $Ce_{1-x}Nd_x$, $Nd_{1-x}Sm_x$) and $LaO_{0.5}F_{0.5}Bi(S_{1-x}Se_x)_2$ systems; however, such a relationship needs to be further confirmed with studies of the effects of in-plane chemical pressure on other BiS_2-based systems. Additional experimental and theoretical efforts are also needed to elucidate the relationship between in-plane chemical pressure and the resultant enhancement of T_c [79].

At present, the highest reported T_c among the BiS_2-based compounds is ~10.7 K for $LaO_{0.5}F_{0.5}BiS_2$ under pressure [30, 80]; however, the BSCCO cuprate superconductors, in which Bi ions are located in the blocking lay-

ers of the structures, can have T_c values higher than 100 K [87–89]. The Ba$_{1-x}$K$_x$BiO$_3$ family, another system containing Bi ions, was reported to have T_c values as high as $\sim$30 K and the BiO$_2$ planes are regarded to be essential for the superconductivity in the compounds [90, 91]. The speed at which new members of BiS$_2$-based superconductors are being synthesized and studied holds promise for the discovery of new superconducting compounds with values of T_c significantly higher than 11 K. Nevertheless, some challenging but essential problems regarding the intrinsic behavior of the BiS$_2$-based superconductors remain to be solved. As the debate over the nature of the pairing mechanism for superconductivity in the BiS$_2$-based superconductors continues, it is difficult to develop an effective strategy for enhancing T_c. The intrinsic transport and thermal properties, which may shed light on the nature of the pairing mechanism, need to be established through further studies on high quality single-crystalline samples. Theoretical calculations, which investigate electronic structure and related properties of BiS$_2$-based superconductors, should be more focused on the actual chemical compositions of the compounds. Another interesting but unclarified issue is the remarkable difference in T_c between the AG and HP annealed samples of Ln(O,F)BiS$_2$ (Ln = La, Ce, Pr). The similarity in both chemical composition and crystal structure of the HP annealed samples and their AG counterparts suggests that the local environment of the crystals may play an essential role in the superconductivity of these BiS$_2$-based compounds. It is hopeful that T_c values for the family of BiS$_2$-based superconductors can be further enhanced if the factors responsible for an increase in T_c such as those affected by HP annealing and the application of external pressure are clarified. Amidst the abundance of physical phenomena thus far observed, at this early stage of discovery and research, there remain unanswered questions and opportunities to develop a fundamental understanding of superconductivity in the BiS$_2$-based compounds.

References

[1] J. G. Bednorz, K. A. Müller, *Z. Phys. B: Condens. Matter* **64**, 189 (1986).
[2] A. P. Drozdov, M. I. Eremets, I. A. Troyan, V. Ksenofontov, S. I. Shylin, *Nature* **525**, 73 (2015).
[3] Y. Mizuguchi, *et al.*, *Phys. Rev. B* **86**, 220510 (2012).
[4] Y. Kamihara, T. Watanabe, M. Hirano, H. Hosono, *J. Am. Chem. Soc.* **130**, 3296 (2008).
[5] G. F. Chen, *et al.*, *Phys. Rev. Lett.* **100**, 247002 (2008).
[6] Z. A. Ren, *et al.*, *Chin. Phys. Lett.* **25**, 2215 (2008).
[7] Z. A. Ren, *et al.*, *Mater. Res. Innovations* **12**, 105 (2008).
[8] Z. Ren, *et al.*, *Europhys. Lett.* **83**, 17002 (2008).
[9] X. H. Chen, T. Wu, R. H. Liu, H. Chen, D. F. Fang, *Nature* **453**, 761 (2008).
[10] J. Xing, S. Li, X. X. Ding, H. Yang, H.-H. Wen, *Phys. Rev. B* **86**, 214518 (2012).
[11] A. S. Sefat, *et al.*, *Phys. Rev. B* **78**, 104505 (2008).
[12] H.-H. Wen, G. Mu, L. Fang, H. Yang, Y. Zhu, *Europhys. Lett.* **82**, 17009 (2008).
[13] C. Wang, *et al.*, *Europhys. Lett.* **83**, 67006 (2008).
[14] Z. A. Ren, *et al.*, *Europhys. Lett.* **83**, 17002 (2008).
[15] J. Yang, *et al.*, *Supercond. Sci. Technol.* **21**, 082001 (2008).
[16] T. Yildirim, *Phys. Rev. B* **87**, 020506 (2013).
[17] J. Shao, *et al.*, *Phys. Status Solidi RRL* **8**, 845 (2014).
[18] V. P. S. Awana, *et al.*, *Solid State Commun.* **157**, 21 (2013).
[19] S. Demura, *et al.*, *J. Phys. Soc. Jpn.* **82**, 033708 (2013).
[20] Y. Mizuguchi, *et al.*, *J. Phys. Soc. Jpn.* **81**, 114725 (2012).
[21] D. Yazici, *et al.*, *Phil. Mag.* **93**, 673 (2013).
[22] Y. Mizuguchi, *Physics Procedia* **58**, 94 (2014).
[23] H. F. Zhai, *et al.*, *Phys. Rev. B* **90**, 064518 (2014).
[24] K. Deguchi, *et al.*, *Europhys. Lett.* **101**, 17004 (2013).
[25] D. Yazici, *et al.*, *Phys. Rev. B* **87**, 174512 (2013).
[26] X. Lin, *et al.*, *Phy. Rev. B* **87**, 020504 (2013).
[27] H. Kotegawa, *et al.*, *J. Phys. Soc. Jpn.* **81**, 103702 (2012).
[28] R. Jha, B. Tiwari, V. P. S. Awana, *J. Phys. Soc. Jpn.* **83**, 105001 (2014).
[29] C. T. Wolowiec, *et al.*, *J. Phys.: Condens. Matter* **25**, 422201 (2013).
[30] C. T. Wolowiec, D. Yazici, B. D. White, K. Huang, M. B. Maple, *Phys. Rev. B* **88**, 064503 (2013).
[31] R. Jha, B. Tiwari, V. P. S. Awana, *J. Phys. Soc. Jpn.* **83**, 063707 (2014).
[32] C. Y. Guo, *et al.*, *Phys. Rev B* **91**, 214512 (2015).
[33] Y. K. Luo, *et al.*, *Phys. Rev. B* **90**, 220510 (2014).
[34] M. Fujioka, *et al.*, *Europhys. Lett.* **108**, 47007 (2014).
[35] S. K. Singh, *et al.*, *J. Am. Chem. Soc.* **134**, 16504 (2012).
[36] Y. Mizuguchi, *J. Phys. Chem. Solids* **84**, 34 (2015).
[37] Y. Yu, J. F. Shao, S. Tan, C. J. Zhang, Y. H. Zhang, *J. Phys. Soc. Jpn.* **82**, 034718 (2013).
[38] R. Jha, V. P. S. Awana, *Physica C* **498**, 45 (2014).
[39] N. R. Werthamer, E. Helfand, P. C. Hohenberg, *Phys. Rev.* **147**, 295 (1966).
[40] S. G. Tan, *et al.*, *Eur. Phys. J. B* **85**, 1 (2012).
[41] Y. Fang, D. Yazici, B. D. White, M. B. Maple, *Phys. Rev. B* **91**, 064510 (2015).
[42] I. Jeon, D. Yazici, B. D. White, A. J. Friedman, M. B. Maple, *Phys. Rev. B* **90**, 054510 (2014).
[43] Z. R. Ye, *et al.*, *Phys. Rev. B* **90**, 045116 (2014).

[44] K. Kuroki, *JPSJ News and Comments* **11**, 02 (2014).

[45] R. Higashinaka, R. Miyazaki, Y. Mizuguchi, O. Miura, Y. Aoki, *J. Phys. Soc. Jpn.* **83**, 5004 (2014).

[46] S. Demura, *et al.*, *J. Phys. Soc. Jpn.* **84**, 024709 (2015).

[47] R. Jha, H. Kishan, V. P. S. Awana, *J. Appl. Phys.* **115**, 013902 (2014).

[48] R. Jha, V. P. S. Awana, *Mater. Res. Express* **1**, 016002 (2014).

[49] C. Morice, *et al.*, *arXiv preprint arXiv:1312.2615* (2013).

[50] H. Usui, K. Suzuki, K. Kuroki, *Phys. Rev. B* **86**, 220501 (2012).

[51] B. Li, Z. W. Xing, G. Q. Huang, *Europhys. Lett.* **101**, 47002 (2013).

[52] J. Lee, *et al.*, *Phys. Rev. B* **87**, 205134 (2013).

[53] Shruti, P. Srivastava, S. Patnaik, *J. Phys.: Condens. Matt.* **25**, 312202 (2013).

[54] G. Lamura, *et al.*, *Phys. Rev. B* **88**, 180509 (2013).

[55] L. Jiao, *et al.*, *J. Phys.: Condens. Matt.* **27**, 225701 (2015).

[56] P. K. Biswas, *et al.*, *Phys. Rev. B* **88**, 224515 (2013).

[57] X. G. Wan, H. C. Ding, S. Y. Savrasov, C. G. Duan, *Phys. Rev. B* **87**, 115124 (2013).

[58] G. B. Martins, A. Moreo, E. Dagotto, *Phys. Rev. B* **87**, 081102 (2013).

[59] Y. Yang, W.-S. Wang, Y.-Y. Xiang, Z.-Z. Li, Q.-H. Wang, *Phys. Rev. B* **88**, 094519 (2013).

[60] Y. Liang, X. Wu, W.-F. Tsai, J. Hu, *Frontiers Phys.* **9**, 194 (2014).

[61] X. Wu, J. Yuan, Y. Liang, H. Fan, J. Hu, *Europhys. Lett.* **108**, 27006 (2014).

[62] T. Zhou, Z. D. Wang, *J. Supercond. Nov. Magn.* **26**, 2735 (2013).

[63] S. Li, *et al.*, *Sci. China: Phys., Mech. Astron.* **56**, 2019 (2013).

[64] J. Z. Liu, *et al.*, *Europhys. Lett.* **106**, 67002 (2014).

[65] J. Kajitani, *et al.*, *Solid State Commun.* **181**, 1 (2014).

[66] E. Paris, *et al.*, *J. Phys.: Condens. Matt.* **26**, 435701 (2014).

[67] A. Miura, *et al.*, *J. Solid State Chem.* **212**, 213 (2014).

[68] A. Miura, *et al.*, *Cryst. Growth Des.* **15**, 39 (2014).

[69] T. Sugimoto, *et al.*, *Phys. Rev. B* **89**, 201117 (2014).

[70] J. Kajitani, T. Hiroi, A. Omachi, O. Miura, Y. Mizuguchi, *J. Supercond. Nov. Magn.* **28**, 1129 (2015).

[71] J. Kajitani, *et al.*, *J. Phys. Soc. Jpn.* **83**, 065002 (2014).

[72] M. Nagao, *et al.*, *Solid State Commun.* **178**, 33 (2014).

[73] M. Nagao, *et al.*, *J. Phys. Soc. Jpn.* **82**, 113701 (2013).

[74] D. Yazici, I. Jeon, B. D. White, M. B. Maple, *Physica C* **514**, 218 (2015).

[75] H. J. Chen, *et al.*, *Inorg. Chem.* **53**, 9 (2013).

[76] G. S. Thakur, *et al.*, *Inorg. Chem.* **54**, 1076 (2015).

[77] J. Kajitani, A. Omachi, T. Hiroi, O. Miura, Y. Mizuguchi, *Physica C* **504**, 33 (2014).

[78] J. Kajitani, T. Hiroi, A. Omachi, O. Miura, Y. Mizuguchi, *J. Phys. Soc. Jpn.* **84**, 044712 (2015).

[79] Y. Mizuguchi, *et al.*, *Sci. Rep.* **5**, 14968 (2015).

[80] T. Tomita, *et al.*, *J. Phys. Soc. Jpn.* **83**, 063704 (2014).

[81] Y. Fang, D. Yazici, B. D. White, M. B. Maple, *Phys. Rev. B* **92**, 094507 (2015).

[82] M. Fujioka, *et al.*, *Appl. Phys. Lett.* **105**, 052601 (2014).

[83] A. Krzton-Maziopa, *et al.*, *J. Phys: Condens. Matter* **26**, 215702 (2014).

[84] T. Hiroi, J. Kajitani, A. Omachi, O. Miura, Y. Mizuguchi, *J. Supercond. Nov. Magn.* **28**, 1149 (2015).

[85] T. Hiroi, J. Kajitani, A. Omachi, O. Miura, Y. Mizuguchi, *J. Phys. Soc. Jpn.* **84**, 024723 (2015).

[86] V. S. Tanryverdiev, O. M. Aliev, I. I. Aliev, *Inorg. Mater.* **31** (1995).

[87] H. Maeda, Y. Tanaka, M. Fukutomi, T. Asano, *Jpn. J. Appl. Phys.* **27**, L209 (1988).

[88] M. A. Subramanian, *et al.*, *Science* **239**, 1015 (1988).

[89] J. L. Tallon, *et al.*, *Nature* **333**, 153 (1988).

[90] R. J. Cava, *et al.*, *Nature* **332**, 814 (1988).

[91] L. F. Mattheiss, D. R. Hamann, *Phys. Rev. Lett.* **60**, 2681 (1988).